

# Quasi-Transient Adjoint Optimization for Vehicle External Aerodynamics

Eugene de Villiers<sup>1)</sup> Andrew Mosedale<sup>2)</sup> Todd Johansen<sup>2)</sup> Georgios Karpouzas<sup>1)</sup>

*1) Engys Ltd., Studio 20, RVPB, John Archer Way, London, SW18 3SX, U.K.*

*(E-mail: e.devilliers@engys.com)*

*2) Auto Research Center, 4012 Championship Dr, Indianapolis, IN 4626, U.S.A.*

**ABSTRACT:** There has been rapidly increasing interest in both the use of transient simulations and the use of the adjoint method to improve the accuracy and efficiency of the design cycle in automotive applications. An approach that draws on both these technologies is evaluated on numerous vehicles. Previous work on the use of adjoint sensitivities has been limited to steady-state approximations, limiting their range of application. The quasi-transient approach has been presented before but is now in practical use for a wide variety of complex design problems. The differences between steady-state and quasi-transient adjoint results are presented for these different vehicles, and the improvements are validated through both physical testing and simulation.

**KEY WORDS:** Heat • Fluid, Aerodynamic Performance, Optimization, Detached Eddy simulation, Adjoint (D1)

## 1. INTRODUCTION

The process of automotive design has been in constant evolution as market demands have changed, and the recent trend towards greater fuel efficiency has increasingly driven the focus on to aerodynamics. This need has been met through the parallel growth of the Computational Fluid Dynamics (CFD) field. In combination with physical testing, CFD has been applied in a variety of ways to improve the design cycle of the product – and the technological nature of CFD has allowed for constant innovation in its application to the Automotive field.

The challenge in the aerodynamic development of a vehicle is often in the interplay between different departments to satisfy different goals. This requires multiple iterations of design which can become costly and time-consuming. In addition, there are often too many coupled parameters to properly evaluate the overall effect of any given change, leading to sub-optimal solutions. Performing such conceptual CFD analysis in the early stages of design can lead to significant savings throughout the product life cycle, but traditional approaches can be unwieldy to set up and can fail to cover the most sensitive areas. Due to advances in processing power, an increasing number of theoretical techniques, such as the Adjoint method, have recently become feasible in industrial scenarios.

Traditionally, CFD was carried out using steady-state models such as the Reynold's Averaged Navier-Stokes (RANS) approach. This reduced the computational cost and allowed for over-stabilization of the solution by approximating the effects of turbulence with a simple set of equations. A lot of research has been done on improving RANS methods and their use in

industrial application has become quite sophisticated and so they were a natural starting point for the development of an Adjoint solver. Simply put, the Adjoint approach posits the existence of a function that can evaluate a certain objective with respect to a surface geometry. By differentiating these equations, the sensitivity of the desired objective to displacement of the surface can be evaluated. While advanced optimisation methods have been applied to automotive cases, they are typically restrained by resource as the number of sample points, hence simulations, required increases proportional to the number of parameters. In addition, setting up a study using eg. Response Surface Methodology (RSM) with parameterised geometry input can be time-consuming and complex. By contrast, the number of Adjoint equations to be solved is proportional only to the number of objectives and is independent of the number of parameters. This makes evaluating adjoint sensitivities an attractive option that is applicable both at early conceptual design stages and also for fine detail optimisation of a productionised vehicle.

Steady-state Adjoint solvers have been increasingly used in a wide-range of applications, especially with the implementation of the second-order accuracy presented last year. However they are still limited by the accuracy of the input flow field, and the fact that key areas of most vehicles exhibit unsteady, transient flow features. An efficient compromise in the industrial solution of these transient cases is to use Detached Eddy Simulation (DES). This approach seeks to fully resolve the turbulent eddies driving the flow in separated regions, while transitioning to RANS modeling near the wall. This allows for a more correct feedback in the pressure field from the wake region behind the

vehicle in particular, and is considered necessary for accurately predicted separation, and so forces, in such bluff-body applications. Fully implementing the Adjoint approach in a transient framework would be extremely costly, however an approximation can be made by using the calculated mean flow of a DES simulation as the input for the adjoint equations<sup>(1)</sup>.

## 2. METHODOLOGY

### 2.1. Steady-State Adjoint

This approach has been tested on a range of vehicle types and is in the process of being validated against experimental testing. Prior experience with the steady-state adjoint has shown that the correlation between the predicted behaviour and physical testing is notably poorer in regions identified as dominated by transient flow effects. These areas tend to show reversed trends when the quasi-transient adjoint is applied, while matching trends in regions of steady flow.

We briefly describe both methodologies to provide a context for the following analysis. The steady state ‘‘primal’’ flow is described by the RANS equations.

$$R^p = -\frac{\partial v_i}{\partial x_i} = 0 \quad (1)$$

$$R_i^v = v_j \frac{\partial v_i}{\partial x_j} + \frac{\partial p}{\partial x_j} - \frac{\partial}{\partial x_j} \left[ (v + v_t) \left( \frac{\partial v_i}{\partial x_j} + \frac{\partial v_j}{\partial x_i} \right) \right] = 0 \quad (2)$$

$$R_i^z = \text{Convection} + \text{Diffusion} + \text{Production} + \text{Disipation} = 0 \quad (3)$$

where  $v_i$  is the primal velocity,  $p$  is the primal pressure,  $v$  and  $v_t$  are the kinematic and turbulent kinematic viscosity, respectively.  $R_i^z$  is considered to be any turbulence model with  $z_i$  representing the multicomponent turbulence vector.

Now, in order to derive the adjoint equations, let us start by defining an objective function  $F$ . The objective can be defined as a combination of surface and volume integrals.

$$F = \int_S F_s dS + \int_\Omega F_\Omega d\Omega \quad (4)$$

$F$  is then augmented (extended) by the state equations,  $R^p$  and  $R_i^v$ .  $F_{aug}$  has different expression from  $F$  but they have the same value, since the residuals  $R$  are zero.

$$F_{aug} = F + \int_\Omega q R^p d\Omega + \int_\Omega u_i R_i^v d\Omega \quad (5)$$

Here,  $q$  and  $u_i$  are the adjoint variables and due to the way they enter the solution algorithm can be interpreted as ‘‘adjoint pressure’’ and ‘‘adjoint velocity’’, respectively. In this example, derivation, the turbulent kinematic viscosity ( $v_t$ ) is assumed constant with respect to changes in the design variables (frozen turbulence assumption).

Differentiating the augmented cost function,  $F_{aug}$ , (see<sup>(3)</sup> for details) produces the adjoint equations for incompressible flow with frozen turbulence:

$$R_\Omega^q = \frac{\partial u_i}{\partial x_i} - \frac{\partial F}{\partial p} = 0 \quad (6)$$

$$R_{i\Omega}^u = -v_j \frac{\partial u_i}{\partial x_j} + u_j \frac{\partial v_j}{\partial x_i} + \frac{\partial q}{\partial x_j}$$

$$-\frac{\partial}{\partial x_j} \left[ (v + v_t) \left( \frac{\partial u_i}{\partial x_j} + \frac{\partial u_j}{\partial x_i} \right) \right] + \frac{\partial F}{\partial v_i} = 0 \quad (7)$$

After solving the adjoint equations, the surface sensitivities of the objective function with respect to the surface normal motion of the surface nodes (design variables) can be calculated with the following expression:

$$\frac{\delta F_{aug}}{\delta b} = - \int_{S_w} \left[ (v + v_t) \left( \frac{\partial u_i}{\partial x_j} + \frac{\partial u_j}{\partial x_i} \right) - q n_i \right] \frac{\partial v_j}{\partial x_k} \frac{\partial x_k}{\partial b_m} dS \quad (8)$$

In shape optimization problems, the surface sensitivities are used as an input to a deformation tool, which morphs the computational domain.

### 2.2. Quasi-Transient Adjoint

The DES (Detached Eddy Simulation) method is an approach that directly resolves most of the important scales of motion rather than approximating these scales with a turbulence model. Due to the reduced modelling dependence, it can be much more accurate and consistently accurate than any RANS based method. The method is however inherently transient and as mentioned previously, transient adjoint is much more costly and cumbersome to evaluate than the steady equivalent. If we are

however, only interested in the time averaged aerodynamic properties of the vehicle, i.e. the mean drag, then an interesting possibility presents itself: to formulate a steady adjoint for the time averaged transient primal flow.

The whole idea of the method is to average the DES primal equations and then calculate the sensitivities by using a steady-state adjoint equation (see<sup>(1)</sup> for details). The algorithm constitutes the following steps:

1. The primal flow variables are calculated by solving LES/DES incompressible Navier-Stokes equations:

$$R^p = -\frac{\partial \bar{v}_i}{\partial x_i} = 0 \quad (9)$$

$$\frac{\partial \bar{v}_i}{\partial t} + \frac{\partial \bar{v}_i \bar{v}_j}{\partial x_j} + \frac{\partial \bar{p}}{\partial x_j} \quad (10)$$

$$-\frac{\partial}{\partial x_j} \left[ (v + v_{SGS}) \left( \frac{\partial \bar{v}_i}{\partial x_j} + \frac{\partial \bar{v}_j}{\partial x_i} \right) \right] = 0$$

The over-bar denotes a spatial filtering operation and  $v_{SGS}$  represents the sub-grid scale turbulence viscosity.

2. During the solution of the primal problem, the required quantities for the adjoint equations are averaged.
3. A new  $v_t^{RAS}$  field is calculated by solving a RAS Spallart-Allmaras equation. In this equation, the mean quantities  $\widehat{v}_i, \widehat{p}, \widehat{phi}$  are used. The  $phi$  denotes the primal velocity flux.
4. The steady state adjoint equations (eqs. (6-7)) are formed by using the mean primal fields and the  $v_t^{RAS}$ .
5. After solving the adjoint equation, the sensitivities are calculated (eq. 8).

### 3. RESULTS

As discussed in Section 2, the sensitivities illustrate the local gradient of the objective function with respect to displacement normal to the surface. In the results shown here, Red indicates a positive gradient - implying that the objective will be improved by pulling out on the surface. Blue indicates a negative gradient, and so to improve the objective the surface must be pushed in. Different objectives can be specified, but in these cases, the desired objective is minimizing the drag force of the whole vehicle.

#### 3.1. Sedan

The first example presented here is the DrivAer notch-back model with detailed underbody<sup>(2)</sup>. An initial comparison of the adjoint sensitivities produced by the previous RANS-based solver and the newer quasi-transient approach shows a large degree of similarity. This is to be expected as much of the flow is steady and is therefore accurately predicted in both approaches.

A particular strength of the adjoint method in design is in the local detail information it can provide however, and so small differences are significant and reflect the more accurate flow representation of the quasi-transient solver. Figure 1 shows such an instance on the rear screen, with the flow over the C-pillars. While both sensitivities advocate for pushing the surface inwards to reduce drag, the focal point is different, with the quasi-transient result showing greater sensitivity at the top of the pillar where the A-pillar vortex interacts with the trailing edge of the roof.



Fig. 1a Overall drag sensitivity to normal displacement of the surface based on the steady-state (SS) adjoint.



Fig. 1b Overall drag sensitivity to normal displacement of the surface based on the quasi-transient (QT) adjoint.

Furthermore, it is worth noting that the sensitivity of the rear of the car is very similar in both pictures. The rear corner is sharp in this design, giving a well-defined separation point. This is a particularly key area in efficient vehicle design, and with more gently curved rear ends, the transient nature of the separation point typically leads to more significant differences and reversed trends between the steady-state and quasi-transient solvers as can be seen in the next example

### 3.2. Pickup Truck

This case studies the sensitivities of a partially simplified pickup truck model. The comparison in Fig. 2 shows the rear corner of the vehicle. The steady-state adjoint shows strong sensitivity to pulling out on the surface on the whole upper section, which can be interpreted as sharpening the corner, presumably to address the separation that can be visualized in Fig. 3 and so improve the base pressure of the vehicle, and reduce drag. By contrast, the quasi-transient sensitivities show a more nuanced response. It favours pulling out the surface on the light cluster, but above that there is a switch in the trend, suggesting a flatter surface with a specific taper in that location would be an improvement on the existing radius. Accurate estimation of the location of the separation on the rear corner is clearly necessary to be able to best control it and achieve maximum possible pressure recovery on the rear face.



Fig. 2 Drag sensitivities for the pickup truck using the SS solver (left) and QT solver (right).

The surface sensitivity maps were exported and used as a factor to morphing the geometry. The preferred process currently involves filtering the sensitivity field in a particular area so that it can be used as a smooth weighting function which is multiplied by the surface normal vector. The triangulated surface can then be warped directly as a post-processing step – in this case up to a maximum of 5mm displacement. This approach can speed up

assessment of design potential and is appropriate in the early stages of development, but cleaner results can be achieved if CAD is available to be morphed directly.

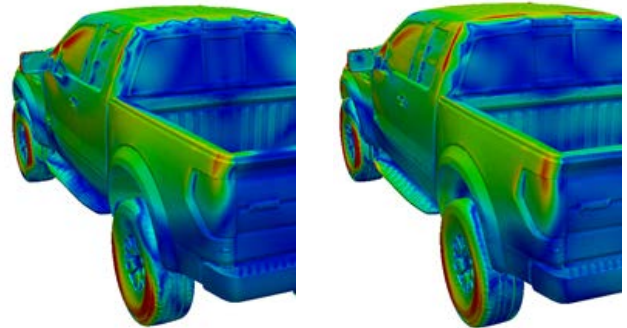


Fig. 3 Near-wall velocities showing the subtle differences in flow separation between the RANS primal (left) and the DES primal (right).

Using DES simulation the results of morphing just the sensitive section of rear corner were a reduction in drag coefficient of 4 counts (~1%). This is based on the quasi-transient sensitivity. Though similar, the steady-state sensitivity based morphing only gave a reduction of 1 count in this area. An additional run with the QT map and a peak deformation of only 3mm found a drag reduction of 2 counts. Although the sensitivity gradient is only valid locally at the surface, there is typically a strong correlation between the strength of the sensitivity and the optimal magnitude of displacement.



Fig. 4 Drag sensitivities for the pickup truck using the QT solver

A similar scenario is seen on the rear of the cab. Here both results indicates that the c-pillar should be pushed in to remove the edge, but the steady-state also shows sensitivity to pulling out at the very trailing edge of the cab. This would lead to a different

angle of taper from the quasi-transient solution, suggestive of a difference in the magnitude of adverse pressure gradient that can be sustained in each solver without separation.

Figure 4 shows the sensitivity at the front of the vehicle, in particular the area around the base of the mirror. This is conventionally a challenging area to optimize due to the interactions of multiple flow phenomena. However, the same process as applied on the rear corners yielded a further 4 count reduction in drag from local changes to the a-pillar immediately in front of the mirror stalk. A third validation run combining several other sensitive areas that would could practically be modified found further gains, and overall led to a total drag reduction of ~2.5% at the cost of a single quasi-transient adjoint run as shown in Table 1.

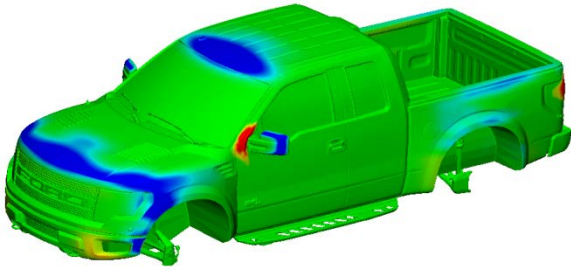


Fig. 5 Areas morphed to give 2.4% drag improvement based on sensitivities of QT solver

### 3.3. Semi-Tractor Trailer

Fuel economy is a particular focus for long-distance trucking, and aerodynamic additions to improve the drag of both tractor and trailer are increasingly common. These parts, such as side-skirts, are in constant development and again the Adjoint method offers insight into potential modifications to optimize the performance of these parts.



Fig. 6a Drag sensitivities on the side-skirts for a tractor-trailer for SS (top) and QT (bottom) solutions.

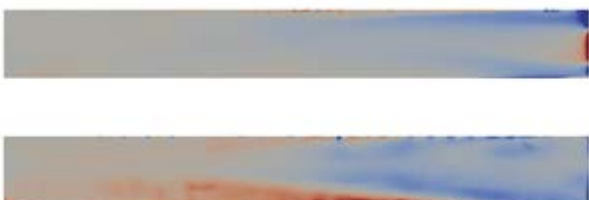


Fig. 6b Closer view of the side-skirt results from SS (top) and QT (bottom) adjoint.

The results shown in in Figure 6 focus on the sensitivities on the side-skirts for a trailer. These devices are typically constant in the vertical dimension, but improvements may be found with a fully 3-dimensional shaped profile. The optimal shape is largely dependent on resolving the turbulent wake from the wheels and tractor underbody, and so notable differences exist between the steady-state and quasi-transient solutions.

A modified skirt was prepared based on the quasi-transient results and allowing for a deflection of up to 15mm. A DES simulation confirmed that this initial attempt already gave a reduction in drag coefficient of 5 counts, a 1% saving which is particularly valuable in the trucking industry.

Vehicle	Adjoint Method	Maximum Morph	Delta Drag Coefficient	Percentage Gain
Pickup	SS	5mm	-0.001	0.2%
Pickup	QT	3mm	-0.002	0.4%
Pickup	QT	5mm (local)	-0.004	0.9%
Pickup	QT	5mm (global)	-0.011	2.4%
Trailer	QT	15mm	-0.005	1%

Table. 1 Summary of improvements found through morphing triangulated surface based on adjoint results.

## 4. CONCLUSION

Examples have shown that the use of the average of a transient flow as an input to the adjoint equations results in different sensitivities to those seen with a more traditional steady-state formulation in areas typically associated with unsteady separation. Specifically, the rear pillars and corners are often significantly different when evaluating drag. Validation based on morphing the triangulated surfaces in the areas identified as highly sensitive found an overall drag reduction of 2.5% on a pick-up truck geometry with practical changes smaller than 5mm. A modified side-skirt for a tractor-trailer was found to give a drag reduction of 1% with a single run. Physical testing to further validate these specific cases is in progress. This approach is extremely cost-effective and holds much potential to streamline all parts of the design process.

## REFERENCES

- (1) G. K. Karpouzas, E. M. Papoutsis-Kiachagias, T. Schumacher, E. de Villiers, K. C. Giannakoglou, C. Othmer: Adjoint Optimization for Vehicle External Aerodynamics, *International Journal of Automotive Engineering*, Vol.7, No.1, pp.1-7(2016) .
- (2) A. Heft, T. Indinger, N. Adams: Introduction of a New Realistic Generic Car Model for Aerodynamic Investigations, *SAE Paper 2012-02-0168*, (2012).
- (3) A.S. Zymaris, D.I. Papadimitriou, K.C. Giannakoglou, C. Othmer: Continuous Adjoint Approach to the Spalart--Allmaras Turbulence Model for Incompressible Flows, *Computers & Fluids*, Vol. 38, Issue 8, p. 1528-1538, (2009).